Wei, J. and Wang, G. (2017) ***Géotechnique Letters* 7**, 161–166, http://dx.doi.org/10.1680/jgele.16.00147

Discrete-element method analysis of initial fabric effects on pre- and post-liquefaction behavior of sands

J. WEI* and G. WANG*

The initial fabric has great influence on the cyclic behaviours of sands. In this study, numerical simulations by the discrete-element method (DEM) were conducted to study the effects of the initial fabric of sands on their cyclic liquefaction resistance and post-liquefaction behaviour. Nine samples with different initial fabric but the same void ratio were prepared by the pre-shearing method, and then subjected to 47 cyclic simple shear tests. The DEM simulation demonstrated that samples with higher degrees of fabric anisotropy have much lower liquefaction resistance compared with an isotropic sample. By incorporating the initial fabric, a single equation can be used to characterise the liquefaction resistance of all the prepared samples. On the other hand, post-liquefaction deformation is not significantly influenced by the initial fabric such that all samples demonstrate similar cyclic behaviour after liquefaction.

KEYWORDS: discrete-element modelling; fabric/structure of soils; liquefaction

NOTATION

- a, b fitting parameters in the cyclic stress ratio (CSR)–N relationship
- a_c degree of anisotropy
- D_r relative density of granular sample
- $E(\Theta)$ angular distribution function of contact normal orientations
- e void ratio of granular sample
- k_1, k_1 fitting parameters in the a–Z relationship
- N number of loading cycles to liquefaction
- N_c total number of inter-particle contacts in the granular sample
- N_p total number of particles in the granular sample
- p_0 initial confining pressure
- Z coordination number
- γ shear strain
- γ_N shear-strain amplitude of the Nth cycle in post-liquefaction stage
- μ_1, μ_2 frictional coefficients of particles at different steps in the pre-shearing method
- μ_{cyc} frictional coefficient of particles during undrained cyclic loading
- σ'_v vertical effective stress
- τ shear stress

INTRODUCTION

The fabric of sands refers to the arrangement of particles, particle groups and pore space distribution (Mitchell & Soga, 2005). It has been found that the fabric may significantly influence the cyclic behaviour of sands, especially liquefaction resistance. Different initial fabric of soil samples can be generated by different sample preparation methods (dry deposition against most tamping) or different pre-shearing histories (Mulilis *et al.*, 1977; Vaid *et al.*, 1989; Ishibashi & Capar, 2003; Yimsiri & Soga, 2010; Sze & Yang, 2013). Finn *et al.* (1970) conducted laboratory tests and found that the pre-shearing history could significantly reduce the liquefaction resistance of sands. Tohno & Shamoto (1986) observed that once a sand deposit was liquefied, it may become easier to liquefy again in a smaller subsequent event, although the sand deposit may densify in post-liquefaction reconsolidation. The reduced liquefaction resistance is probably due to the change of fabric by the pre-shearing histories of seismic loading. Similar observations have also been confirmed by other researchers (Nemat-Nasser & Tobita, 1982; Suzuki & Toki, 1984; Oda *et al.*, 2001; Ye *et al.*, 2015, 2016).

However, it is difficult to quantitatively study the soil fabric using existing laboratory techniques. On the other hand, microscopic information on the granular packing can be easily obtained using the discrete-element method (DEM) to quantify the soil fabric (Thornton, 2000; Yimsiri & Soga, 2010; Guo & Zhao, 2013; Wei & Wang, 2016). Several recent studies have proven that DEM is an excellent tool to simulate the cyclic liquefaction and post-liquefaction process of sands, including evolution of the particle-void structure (Wei & Wang, 2014, 2015; Wang & Wei, 2016; Wang *et al.*, 2016). In this study, nine samples with different initial fabric but the same void ratio were prepared by the pre-shearing method in the DEM simulation. Forty-seven cyclic simple shear tests were conducted on the samples to study the influence of initial fabric on the cyclic behaviour of the sand, including liquefaction resistance and shear-strain evolution in the post-liquefaction stage.

NUMERICAL SIMULATION

Quantification of fabric based on inter-particle contacts

In this study, only fabric due to the anisotropic distribution of inter-particle contacts is considered. Fabric associated with particle shape is not considered by using spherical particles in the simulation. The contact-based fabric can be quantified using the following second-order fabric tensor (Oda, 1982; Satake, 1982; Sitharam *et al.*, 2009)

$$\boldsymbol{\Phi}_{ij} = \frac{1}{N_c}\sum_{k=1}^{N_c} n_i^{(k)} n_j^{(k)} = \int_{\Theta} E(\Theta) n_i n_j \, \mathrm{d}\Theta \qquad (1)$$

Manuscript received 12 October 2016; first decision 28 March 2017; accepted 28 March 2017.
Published online at www.geotechniqueletters.com on 24 April 2017.
*Department of Civil and Environmental Engineering, The Hong Kong University of Science and Technology, Clear Water Bay, Kowloon, Hong Kong.

where $\boldsymbol{n}$ is the contact normal vector and N_c is the total number of inter-particle contacts. $E(\Theta)$ is the angular distribution function of contact normal orientations ($\int_\Theta E(\Theta)\,d\Theta = 1$), which can be approximated using Fourier series (Ouadfel & Rothenburg, 2001; Sitharam *et al.*, 2009)

$$E(\Theta) = \frac{1}{4\pi}(1 + \boldsymbol{a}_{ij}n_i n_j) \tag{2}$$

where $\boldsymbol{a}_{ij}$ is a symmetric second-order tensor that contributes to the deviatoric part of the fabric tensor, $\boldsymbol{\phi}'_{ij}$, through the relationship $\boldsymbol{a}_{ij} = (15/2)\boldsymbol{\phi}'_{ij}$. Summation on repeated indices is implied. The invariant of $\boldsymbol{a}_{ij}$, denoted as a_c, is used to quantify the anisotropy degree of the fabric tensor

$$a_c = \sqrt{\frac{3}{2}(\boldsymbol{a}_{ij}\boldsymbol{a}_{ij})} \tag{3}$$

On the other hand, the coordination number ($Z = 2N_c/N_p$, where N_p is the total number of particles) is a useful contact-based fabric, which measures the average number of contacts per particle. The coordination number has been verified as having a strong correlation with the microscopic load-bearing structure in granular packings (Wei & Wang, 2015; Xu *et al.*, 2015; Wang & Wei, 2016; Wang *et al.*, 2016). In this study, both a_c and Z are used as fabric indicators.

Pre-shearing method to prepare samples with different initial fabric

Discrete-element software, Yade (Šmilauer *et al.*, 2010), is applied to perform the numerical simulation. A cubic sample is generated with a total number of 10 000 spherical particles under a periodic boundary (O'Sullivan, 2011), as shown in Fig. 1(a). The radii of the particles range from 0·15 to 0·45 mm according to the grain size distribution in Fig. 1(b), and the particle density is 2650 kg/m^3. A simplified Hertz–Mindlin model (Yimsiri & Soga, 2010) is used to calculate the inter-particle contact forces, with Young's modulus of the solid grains set as 70 GPa and Poisson's ratio as 0·3.

The pre-shearing method (Yimsiri & Soga, 2010) is employed in the numerical simulation to generate samples with different initial fabric but the same void ratio under the same confining pressure. The sample preparation includes three steps. In the first step, the sample is isotropically compressed under a confining pressure $p_0 = 100$ kPa. The frictional coefficient of the particles is assigned as μ_1. The second step is a pre-shearing process to induce fabric anisotropy. The sample is subjected to drained triaxial compression, where the horizontal confinement stresses are maintained at 100 kPa, while the vertical confinement stress increases until the axial strain reaches 2%. The process induces anisotropic fabric in the sample, as the contact normals concentrate along the compression direction (Yimsiri & Soga, 2010). During the pre-shearing process, the frictional coefficient of the particles is assigned as μ_2. In the third step, the sample is unloaded to a hydrostatic state $p_0 = 100$ kPa, with the frictional coefficient of the particles remaining at μ_2 during the step. Finally, the prepared sample is subjected to undrained cyclic simple shear testing to study the liquefaction process, with the frictional coefficient of the particles is assigned as $\mu_{cyc} = 0{\cdot}5$.

To ensure that the samples are stable after the change in the frictional coefficients of the particles in the different steps, the following relationship needs to be satisfied

$$\mu_1 \le \mu_2 \le \mu_{cyc} \tag{4}$$

It is worth mentioning that increasing the frictional coefficient in these subsequent steps will increase the frictional resistance among the contacting particles. Therefore, the load established between the contacting particles and the fabric will not be affected by changing the frictional coefficient. Generally speaking, the frictional coefficient μ_2 controls the anisotropy degree of the fabric tensor (also the coordination number) in the prepared samples. Higher fabric anisotropy can be retained in the prepared sample using a higher value of μ_2 (refer to Table 1). The value of μ_1 can be found by trial and error such that all prepared samples have the same void ratio.

Nine samples with different initial fabric are prepared for cyclic simple shear tests. Sample ISO is an isotropic sample prepared without pre-shearing. Samples S1–S8 are prepared by the pre-shearing method using different values of μ_1 and μ_2. As summarised in Table 1, all the prepared samples have almost identical void ratios under the confining pressure of 100 kPa. These samples are categorised as medium-dense sand since the relative density (D_r) is around 0·56 (maximum and minimum void ratios are 0·759 and 0·497, respectively). In Table 1, the cyclic stress ratio (CSR) is defined as the cyclic shear stress (τ) acting on a horizontal plane divided by the vertical confinement stress ($\sigma'_v = 100$ kPa), CSR $= \tau/\sigma'_v$.

Characterisation of initial fabric in different samples

Fabric indicators a_c and Z are used to characterise the initial fabric of these samples, as shown in Fig. 2. Sample ISO has

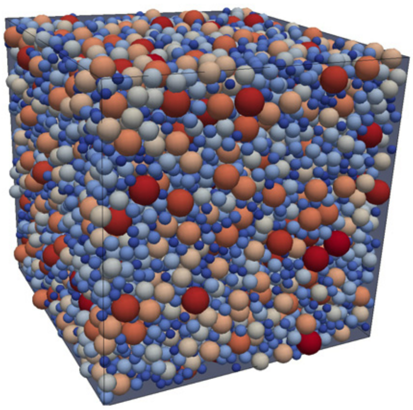

(a)

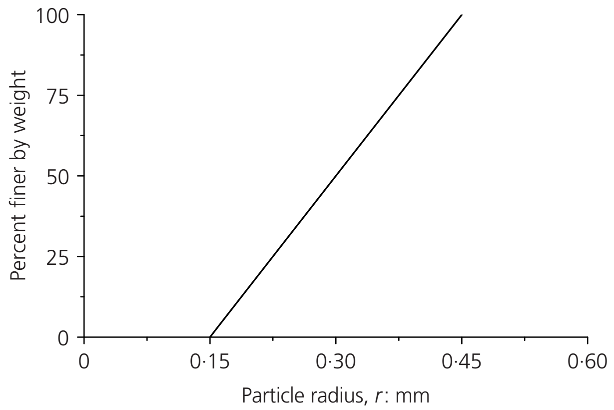

(b)

Fig. 1. Granular packing in the numerical simulation: (a) three-dimensional granular packing and (b) particle size distribution curve

Table 1. Different initial fabric of samples and the following loading conditions

Sample	μ_2	μ_1	Void ratio	CSR during cyclic loading
ISO	—	—	0·6115	0·25/0·30/0·35/0·40/0·45
S1	0·138	0·138	0·6114	0·25/0·30/0·35/0·40/0·45
S2	0·167	0·121	0·6112	0·25/0·30/0·35/0·40/0·45
S3	0·203	0·111	0·6118	0·20/0·25/0·30/0·35/0·40/0·45
S4	0·245	0·105	0·6112	0·15/0·20/0·25/0·30/0·35/0·40
S5	0·288	0·103	0·6119	0·10/0·15/0·20/0·25/0·30/0·35
S6	0·309	0·103	0·6119	0·10/0·15/0·20/0·25/0·30
S7	0·365	0·102	0·6112	0·10/0·15/0·20/0·25/0·30
S8	0·500	0·094	0·6114	0·10/0·15/0·20/0·25

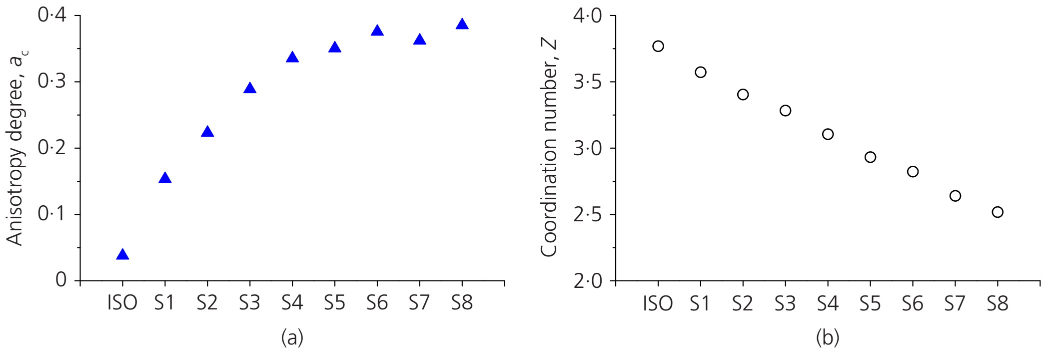

Fig. 2. Fabric indicators: (a) anisotropy degree a_c and (b) coordination number Z

the lowest anisotropy degree of initial fabric ($a_c = 0{\cdot}038$) in Fig. 2(a). a_c increases from 0·15 to 0·38 in samples S1–S8 due to the concentration of the inter-particle contacts along the compression direction.

Coordination numbers Z of these samples are demonstrated in Fig. 2(b). Sample ISO has the highest Z of 3·77. The coordination number gradually decreases from 3·57 to 2·51 in samples S1–S8, which means that the inter-particle contacts become fewer when the anisotropic degree increases, even though the samples are under the same confining pressure. This can also be clearly seen in the force chain networks shown in Fig. 3. The force chain network in S8 has a lower density than that in ISO, yet, the large contact forces become more frequent in S8 compared with that in ISO.

Two more sets of samples with void ratios of 0·65 ($D_r = 0{\cdot}41$) and 0·69 ($D_r = 0{\cdot}25$) are also prepared using the pre-shearing method and the results are shown in Fig. 4. The negative correlation between $a_c$and Z can be observed for all cases.

SIMULATION RESULTS

Liquefaction resistance

Figure 5 shows the stress paths of samples ISO and S6 from the isotropic stress state $p_0 = 100$ kPa to initial liquefaction under undrained cyclic simple shear ($D_r = 0{\cdot}56$, CSR = 0·30). The initial liquefaction is identified when the vertical effective stress is practically zero (smaller than 0·5 kPa). Although the two samples have the same void ratio,

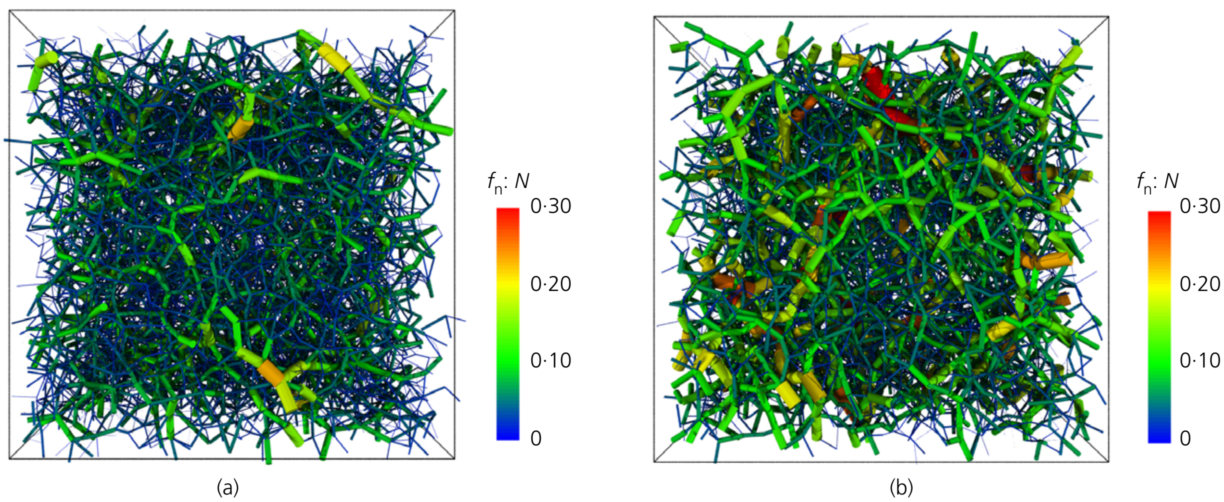

Fig. 3. Force chain networks of samples in: (a) an isotropic sample ISO and (b) a highly anisotropic sample S8. The magnitudes of inter-particle normal contact forces are represented by the thickness of the chains and colour

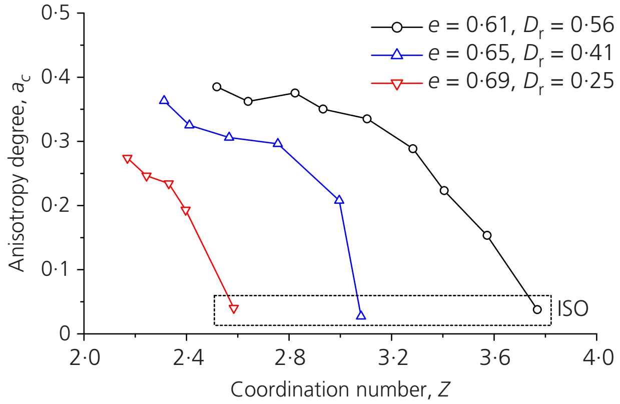

Fig. 4. Relationship between anisotropy degree a_c and coordination number Z of samples for different void ratios

the number of loading cycles to liquefaction differs dramatically. Sample ISO requires 189 loading cycles to reach the initial liquefaction, while liquefaction occurs in sample S6 within four loading cycles. It's obvious that sample ISO has much higher liquefaction resistance compared with sample S6.

According to the test program shown in Table 1, a total number of 47 numerical tests were conducted to study the influence of initial fabric on liquefaction resistance. Figure 6(a) shows the CSR required to reach initial liquefaction against the number of cycles (N) needed. Sample ISO has the highest liquefaction resistance while sample S8 has the lowest liquefaction resistance. The liquefaction resistance curves are almost parallel to each other on a log N–CSR scale. The simulation results are in good agreement with the laboratory test results (Suzuki & Toki, 1984; Oda *et al.*, 2001; Ye *et al.*, 2015) in that the liquefaction resistance decreases dramatically when the soil samples were pre-sheared.

For each sample, the CSR required to reach initial liquefaction (also called cyclic resistance ratio) can be related to the number of cycles (N) by a power function (Idriss & Boulanger, 2008):

$$\text{CSR} = aN^{-b} \tag{5}$$

where a and b are fitting parameters. From the simulation, $b = 0{\cdot}186$ for all samples. The parameter a depends on many factors, including void ratio, initial fabric, confining pressure and so on.

For all the prepared samples (with the same void ratio under the same confining pressure), the parameter a can be related to the coordination number Z by way of the following linear relationship

$$a = k_1 Z - k_2 \tag{6}$$

where $k_1 = 0{\cdot}44$ and $k_2 = 0{\cdot}886$. Figure 6(b) shows all the data can be well fitted by this relationship. Note that the

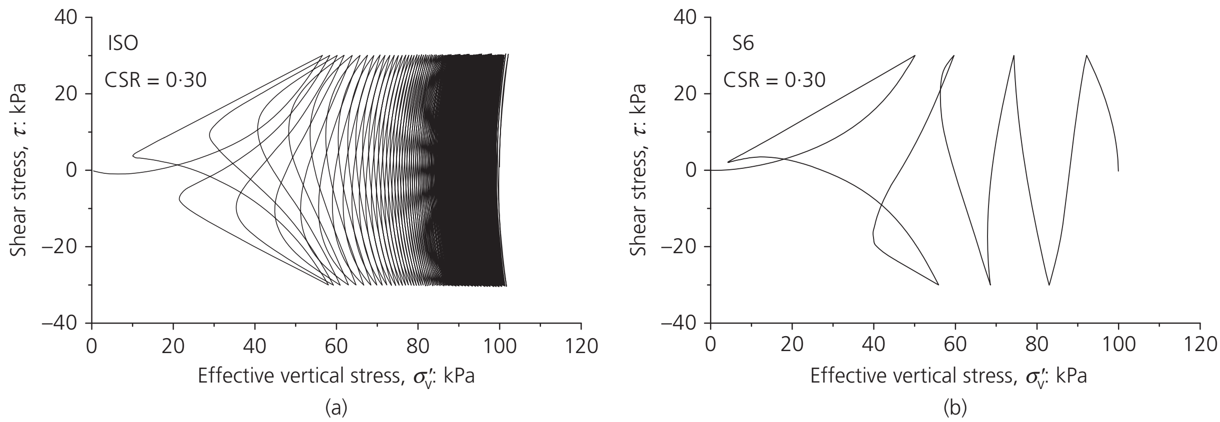

Fig. 5. Stress path of samples with different initial fabric before initial liquefaction and CSR = 0·30 during the cyclic loading: (a) sample ISO and (b) sample S6

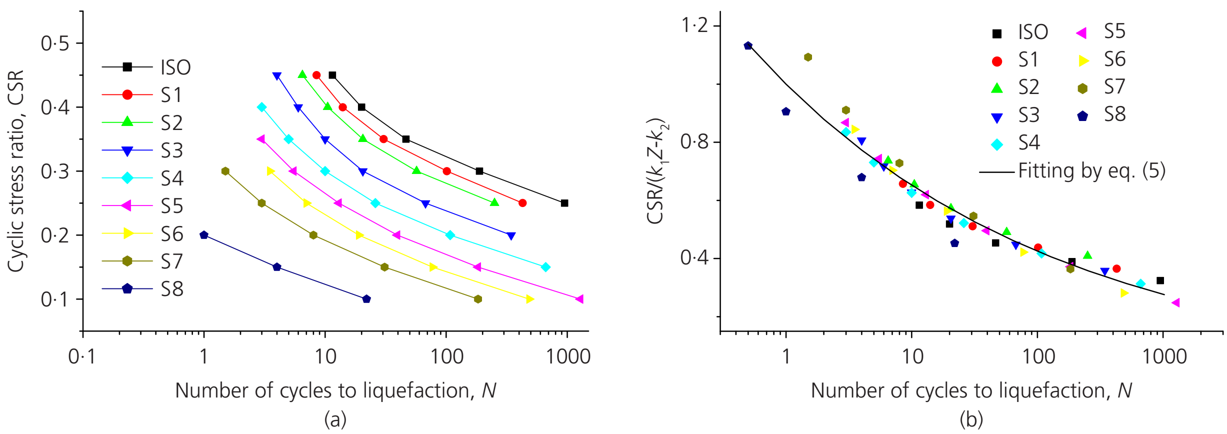

Fig. 6. (a) The CSR required to reach initial liquefaction against the number of cycles for nine samples ($D_r = 0{\cdot}56$) and (b) CSR/($k_1Z - k_2$) against the number of cycles

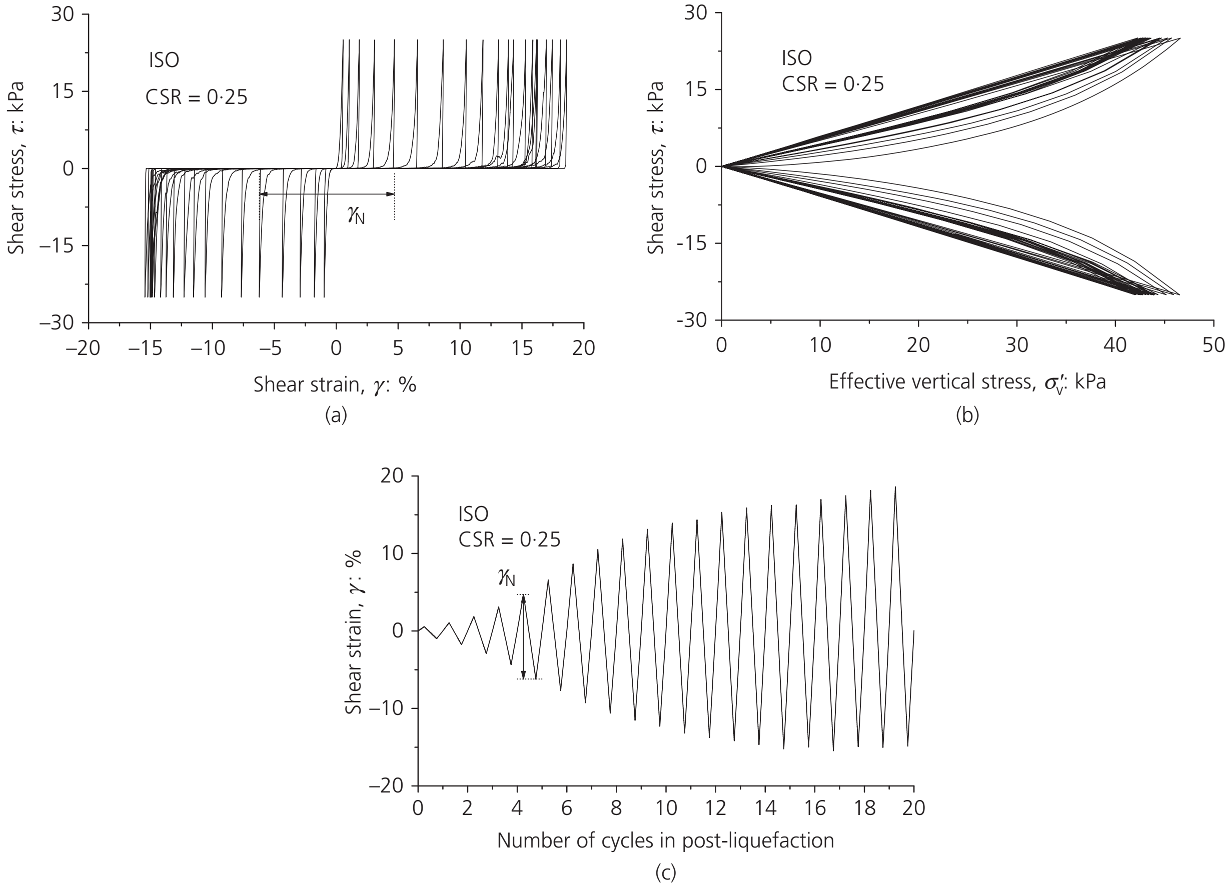

Fig. 7. Response of sample ISO in post-liquefaction stage: (a) stress–strain behaviour; (b) stress path and (c) evolution of shear-strain amplitude with number of cycles in post-liquefaction

above relationship is derived only for samples with $D_r = 0{\cdot}56$; however, a similar functional form may be expected for other densities. In addition, the coordination number Z can be related to anisotropy degree a_c through Fig. 4 for different densities. Therefore, it is also possible to relate the parameter a with a_c or other fabric indicators.

Post-liquefaction behaviour

After liquefaction, the shear-strain amplitude increases rapidly with continued cyclic loading. This phenomenon is called cyclic mobility (Wang & Xie, 2014; Ye & Wang, 2015). Figure 7 demonstrates the behaviour of sample ISO in post-liquefaction with the cyclic shear stress $\tau = 25$ kPa (CSR = 0·25). The number of cycles shown in Fig. 7(c) is counted after the initial liquefaction. The stress path repeats a 'butterfly loop' pattern and the amplitude of the shear strain increases cycle by cycle. The results are qualitatively similar to the experimental observations (Zhang & Wang, 2012). To explore the influence of initial fabric on post-liquefaction behaviour, the evolution of the shear-strain amplitude γ_N is considered. As shown in Fig. 7(c), γ_N increases from <2% in the first cycle to nearly 35% after 20 loading cycles.

The evolution of γ_N in the post-liquefaction stage is summarised in Fig. 8, and is found to be very similar for all cases. γ_N increases rapidly in the first ten cycles and the rate of increase gradually reduces in the subsequent cycles. A slight difference among these curves can be observed in the first several cycles in which γ_N of the sample ISO is lower than the other samples. With more loading cycles, the difference gradually diminishes and γ_N of all samples finally becomes saturated around 30–35%. Compared with the significant difference of the sand behaviour before liquefaction (refer to Fig. 5), the post-liquefaction difference is negligible.

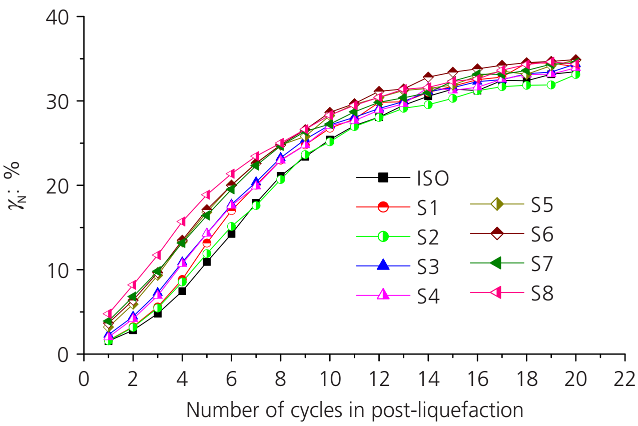

Fig. 8. Shear-strain amplitude γ_N in post-liquefaction loading cycles for samples with different initial fabric

CONCLUSIONS

In this study, the influence of initial fabric on the cyclic behaviour of sands was explored using DEM simulation. Samples with different initial fabric but the same void ratio were prepared by the pre-shearing method. Compared with an isotropic sample (prepared without pre-shearing), samples prepared with pre-shearing have higher fabric anisotropy, associated with a lower coordination number. Results from numerical simulation demonstrate the significant influence of the initial fabric to the liquefaction resistance, which decreases dramatically for samples with higher degrees of anisotropy and lower coordination numbers. Based on DEM simulation, the number of cycles to initial liquefaction for all samples can be characterised using a single equation by incorporating the fabric indicators. On the other hand, all samples demonstrated similar cyclic behaviour after liquefaction, implying that the influence of the initial fabric on the post-liquefaction behaviour is not significant.

ACKNOWLEDGEMENTS

This study was financially supported by Theme-based Research Scheme Grant No. T22-603/15N and General Research Fund No. 16213615 from the Hong Kong Research Grants Council.

REFERENCES

Finn, W., Bransby, P. L. & Pickering, D. J. (1970). Effect of strain history on liquefaction of sand. *J. Soil Mech. Found. Div. ASCE* **96**, No. 6, 1917–1934.

Guo, N. & Zhao, J. (2013). The signature of shear-induced anisotropy in granular media. *Comput. Geotech.* **47**, 1–15, http://doi.org/10.1016/j.compgeo.2012.07.002.

Idriss, I. M. & Boulanger, R. W. (2008). *Soil liquefaction during earthquakes*. Oakland, CA, USA: Earthquake Engineering Research Institute.

Ishibashi, I. & Capar, O. F. (2003). Anisotropy and its relation to liquefaction resistance of granular material. *Soils Found.* **43**, No. 5, 149–159.

Mitchell, J. & Soga, K. (2005). *Fundamentals of soil behavior*, 3rd edn. New York, NY, USA: John Wiley & Sons.

Mulilis, J. P., Arulanandan, K., Mitchell, J. K., Chan, C. K. & Seed, H. B. (1977). Effects of sample preparation on sand liquefaction. *J. Geotech. Engng Div. ASCE* **103**, No. 2, 91–108.

Nemat-Nasser, S. & Tobita, Y. (1982). Influence of fabric on liquefaction and densification potential of cohesionless sand. *Mech. Mater.* **1**, No. 1, 43–62.

Oda, M. (1982). Fabric tensor for discontinuous geological materials. *Soils Found.* **22**, No. 4, 96–108.

Oda, M., Kawamoto, K., Suzuki, K., Fujimori, H. & Sato, M. (2001). Microstructural interpretation on reliquefaction of saturated granular soils under cyclic loading. *J. Geotech. Geoenviron. Engng* **127**, No. 5, 416–423.

O'Sullivan, C. (2011). *Particulate discrete element modelling, a geomechanics perspective*. Oxon, UK: Spon Press.

Ouadfel, H. & Rothenburg, L. (2001). Stress–force–fabric relationship for assemblies of ellipsoids. *Mech. Mater.* **33**, No. 4, 201–221.

Satake, M. (1982). Fabric tensor in granular materials. In *Deformation and failure of granular materials* (eds P. A. Vermeer and H. J. Luger), pp. 63–68. Rotterdam, the Netherlands: Balkema.

Sitharam, T., Vinod, J. & Ravishankar, B. (2009). Post-liquefaction undrained monotonic behaviour of sands: experiments and DEM simulations. *Géotechnique* **59**, No. 9, 739–749, http://dx.doi.org/10.1680/geot.7.00040.

Šmilauer, V., Catalano, E., Chareyre, B., Dorofeenko, S., Duriez, J., Gladky, A., Kozicki, J., Modenese, C., Scholtès, L., Sibille, L., Stránský, J. & Thoeni, K. (2010). *Yade documentation*, 1st edn. See https://www.yade-dem.org/doc/ (accessed 20/04/2017).

Suzuki, T. & Toki, S. (1984). Effects of preshearing on liquefaction characteristics of saturated sand subjected to cyclic loading. *Soils Found.* **24**, No. 2, 16–28.

Sze, H. & Yang, J. (2013). Cyclic loading behavior of saturated sand with different fabrics. In *Proceedings of the 18th international conference on soil mechanics and geotechnical engineering* (eds P. Delage, J. Desrues, R. Frank, A. Puech, F. Schlosser), pp. 1611–1614. Paris, France: Presses des Ponts.

Thornton, C. (2000). Numerical simulations of deviatoric shear deformation of granular media. *Géotechnique* **50**, No. 1, 43–53, http://dx.doi.org/10.1680/geot.2000.50.1.43.

Tohno, I. & Shamoto, Y. (1986). Liquefaction damage to the ground during the 1983 Nihonkai-Chubu (Japan Sea) earthquake in Aomori Prefecture, Tohoku, Japan. *J. Nat. Disaster Sci.* **8**, No. 1, 85–116.

Vaid, Y., Chung, E. & Kuerbis, R. (1989). Preshearing and undrained response of sand. *Soils Found.* **29**, No. 4, 49–61.

Wang, G. & Wei, J. (2016). Microstructure evolution of granular soils in cyclic mobility and post-liquefaction process. *Granular Matter* **18**, No. 3, 51, 1–13.

Wang, G. & Xie, Y. (2014). Modified bounding surface hypoplasticity model for sands under cyclic loading. *J. Engng Mech.* **140**, No. 1, 91–101.

Wang, R., Fu, P., Zhang, J. M. & Dafalias, Y. F. (2016). DEM study of fabric features governing undrained post-liquefaction shear deformation of sand. *Acta Geotech.* **11**, No. 6, 1321–1337.

Wei, J. & Wang, G. (2014). Cyclic mobility and post-liquefaction behaviors of granular soils under cyclic loading: micromechanical perspectives. *Proceedings of the 10th US national conference on earthquake engineering*, Anchorage, AK, USA, paper No. 1501.

Wei, J. & Wang, G. (2015). Evolution of packing structure in cyclic mobility and post-liquefaction of granular soils. In *Bifurcation and degradation of geomaterials in the new millennium (Springer Series in Geomechanics and Geoengineering)* (eds K. T. Chau and J. Zhao), pp. 267–272. Heidelberg, Berlin, Germany: Springer International Publishing.

Wei, J. & Wang, G. (2016). Evolution of fabric anisotropy in cyclic liquefaction of sands. *Journal of Micromechanics and Molecular Physics* **1**, No. 3 & 4, 1640005.

Xu, X. M., Ling, D. S., Cheng, Y. P. & Chen, Y. M. (2015). Correlation between liquefaction resistance and shear wave velocity of granular soils: a micromechanical perspective. *Géotechnique* **65**, No. 5, 337–348, http://dx.doi.org/10.1680/geot.SIP.15.P.022.

Ye, B., Lu, J. & Ye, G. (2015). Pre-shear effect on liquefaction resistance of a Fujian sand. *Soil Dyn. Earthquake Engng* **77**, 15–23, http://doi.org/10.1016/j.soildyn.2015.04.018.

Ye, J. & Wang, G. (2015). Seismic dynamics of offshore breakwater on liquefiable seabed foundation. *Soil Dyn. Earthquake Engng* **76**, 86–99, http://doi.org/10.1016/j.soildyn.2015.02.003.

Ye, J., Huang, D. & Wang, G. (2016). Nonlinear simulation of offshore breakwater on sloping liquefied seabed. *Bull. Engng Geol. Environ.* **75**, No. 3, 1215–1225.

Yimsiri, S. & Soga, K. (2010). DEM analysis of soil fabric effects on behaviour of sand. *Géotechnique* **60**, No. 6, 483–495, http://dx.doi.org/10.1680/geot.2010.60.6.483.

Zhang, J. & Wang, G. (2012). Large post-liquefaction deformation of sand, part I: physical mechanism, constitutive description and numerical algorithm. *Acta Geotech.* **7**, No. 2, 69–113.

HOW CAN YOU CONTRIBUTE?

To discuss this paper, please submit up to 500 words to the editor at journals@ice.org.uk. Your contribution will be forwarded to the author(s) for a reply and, if considered appropriate by the editorial board, it will be published as a discussion in a future issue of the journal.